

Beamtest characterization of the ENUBET Demonstrator^(*)

G. SAIBENE⁽¹⁾⁽²⁾, F. ACERBI⁽³⁾, I. ANGELIS⁽²²⁾, L. BOMBEN⁽¹⁾⁽²⁾, M. BONESINI⁽¹⁾,
F. BRAMATI⁽¹⁾⁽¹²⁾, A. BRANCA⁽¹⁾⁽¹²⁾, C. BRIZZOLARI⁽¹⁾⁽¹²⁾, G. BRUNETTI⁽¹⁾⁽¹²⁾,
M. CALVIANI⁽¹⁷⁾, S. CAPELLI⁽¹⁾⁽²⁾, S. CARTURAN⁽⁴⁾, M. G. CATANESI⁽¹¹⁾,
S. CECCHINI⁽⁷⁾, N. CHARITONIDIS⁽¹⁷⁾, F. CINDOLO⁽⁷⁾, G. COGO⁽¹⁴⁾,
G. COLLAZUOL⁽⁵⁾⁽¹⁴⁾, F. DAL CORSO⁽⁵⁾, C. DELOGU⁽⁵⁾⁽¹⁴⁾, G. DE ROSA⁽¹⁰⁾,
A. FALCONE⁽¹⁾⁽¹²⁾, B. GODDARD⁽¹⁷⁾, A. GOLA⁽³⁾, D. GUFFANTI⁽¹⁾⁽¹²⁾,
L. HALIĆ⁽²¹⁾, F. IACOB⁽⁵⁾⁽¹⁴⁾, M. A. JEBRAMCIK⁽¹⁷⁾, C. JOLLET⁽¹⁹⁾, V. KAIN⁽¹⁷⁾,
A. KALLITSOPOULOU⁽²⁰⁾, B. KLIČEK⁽²¹⁾, Y. KUDENKO⁽¹⁸⁾, CH. LAMPOUDIS⁽²²⁾,
M. LAVEDER⁽⁵⁾⁽¹⁴⁾, P. LEGOU⁽²⁰⁾, A. LONGHIN⁽⁵⁾⁽¹⁴⁾, L. LUDOVICI⁽⁹⁾,
E. LUTSENKO⁽¹⁾⁽²⁾, L. MAGALETTI⁽¹¹⁾⁽¹⁶⁾, G. MANDRIOLI⁽⁷⁾, S. MARANGONI⁽¹⁾⁽¹²⁾,
A. MARGOTTI⁽⁷⁾, V. MASCAGNA⁽¹³⁾⁽⁶⁾, N. MAURI⁽⁷⁾, J. MCELWEE⁽¹⁹⁾,
L. MEAZZA⁽¹⁾⁽¹²⁾, A. MEREGAGLIA⁽¹⁹⁾, M. MEZZETTO⁽⁵⁾, M. NESSI⁽¹⁷⁾,
A. PAOLONI⁽⁸⁾, M. PARI⁽⁵⁾⁽¹⁴⁾, T. PAPAEVANGELOU⁽²⁰⁾, E. G. PAROZZI⁽¹⁾⁽¹²⁾,
L. PASQUALINI⁽⁷⁾⁽¹⁵⁾, G. PATERNOSTER⁽³⁾, L. PATRIZII⁽⁷⁾, M. POZZATO⁽⁷⁾,
M. PREST⁽¹⁾⁽²⁾, F. PUPILLI⁽⁵⁾, E. RADICIONI⁽¹¹⁾, A. C. RUGGERI⁽¹⁰⁾,
D. SAMPSONIDIS⁽²²⁾, C. SCIAN⁽¹⁴⁾, G. SIRRI⁽⁷⁾, M. STIPČEVIĆ⁽²¹⁾, M. TENTI⁽⁷⁾,
F. TERRANOVA⁽¹⁾⁽¹²⁾, M. TORTI⁽¹⁾⁽¹²⁾, S. E. TZAMARIAS⁽²²⁾, E. VALLAZZA⁽¹⁾,
F. VELOTTI⁽¹⁷⁾ and L. VOTANO⁽⁸⁾

⁽¹⁾ INFN, Sezione di Milano-Bicocca - piazza della Scienza 3, Milano, Italy

⁽²⁾ DiSAT, Università degli studi dell'Insubria - via Valleggio 11, Como, Italy

⁽³⁾ Fondazione Bruno Kessler (FBK) and INFN TIFPA - Trento, Italy

⁽⁴⁾ INFN, Laboratori Nazionali di Legnaro - Viale dell'Università 2, Legnaro (PD), Italy

⁽⁵⁾ INFN, Sezione di Padova - via Marzolo 8, Padova, Italy

⁽⁶⁾ INFN, Sezione di Pavia - via Bassi 6, Pavia, Italy

⁽⁷⁾ INFN, Sezione di Bologna - viale Berti-Pichat 6/2, Bologna, Italy

⁽⁸⁾ INFN, Laboratori Nazionali di Frascati - via Fermi 40, Frascati (Rome), Italy

⁽⁹⁾ INFN, Sezione di Roma 1 - piazzale A. Moro 2, Rome, Italy

⁽¹⁰⁾ INFN, Sezione di Napoli - via Cinthia, 80126, Napoli, Italy

⁽¹¹⁾ INFN, Sezione di Bari - via Amendola 173, Bari, Italy

⁽¹²⁾ Dipartimento di Fisica, Università di Milano-Bicocca - piazza della Scienza 3, Milano, Italy

⁽¹³⁾ DII, Università degli studi di Brescia - via Branze 38, Brescia, Italy

⁽¹⁴⁾ Dipartimento di Fisica, Università di Padova - via Marzolo 8, Padova, Italy

⁽¹⁵⁾ Dipartimento di Fisica, Università di Bologna, viale Berti-Pichat 6/2, Bologna, Italy

⁽¹⁶⁾ Dipartimento di Fisica, Università degli Studi di Bari - via Amendola 173, Bari, Italy

⁽¹⁷⁾ CERN - Geneva, Switzerland

⁽¹⁸⁾ Institute of Nuclear Research of the Russian Academy of Science - Moscow, Russia

⁽¹⁹⁾ LP2I Bordeaux, Université de Bordeaux, CNRS/IN2P3 - 33175 Gradignan, France

⁽²⁰⁾ CEA, Centre de Saclay, Irfu/SPP - F-91191 Gif-sur-Yvette, France

⁽²¹⁾ Center of Excellence for Advanced Materials and Sensing Devices, Ruder Boskovic Institute HR-10000 Zagreb, Croatia

⁽²²⁾ Aristotle University of Thessaloniki - Thessaloniki 541 24, Greece

^(*) IFAE 2024 - "New Technologies" session

received 2 December 2024

Summary. — The goal of the ENUBET project is to develop the first *monitored neutrino beam*, where the neutrino flux can be measured with a 1% precision, in order to carry out measurements of high precision of the neutrino cross section in the energy range of relevance for HyperKamiokande and DUNE. The systematic uncertainties are suppressed by detecting, in an instrumented decay tunnel, the large-angle leptons generated in the K_{e3}^+ three body decay ($K^+ \rightarrow e^+ \pi^0 \nu_e$). The collaboration recently completed the beamline design and tested the largest prototype of the decay tunnel: the Demonstrator. It is a sampling calorimeter composed of iron absorbers and plastic scintillators, whose light is collected by WLS fibers and readout by SiPMs. In this contribution, we discuss the characterization results obtained in the two beamtests on the PS extracted T9 beamline at CERN in 2022 and 2023. Namely the linearity and energy resolution, the effect of the optical crosstalk and a first preliminary particle identification analysis.

1. – Introduction

The Standard Model (SM) of particle physics combines the description of the electrodynamics, the weak interactions and the strong interactions with the classification of all the known elementary particles. Neutrinos are the least known fermions of the SM. Indeed, this is not related to the rarity of neutrinos, but to their interaction with matter. As any other lepton, they do not experience strong interactions, and, having no electric charge, these particles interact only through the weak force. Thus, experimental neutrino physics is quite challenging. Moreover, neutrinos are key ingredients for Beyond SM searches and still a source of unexpected results [1].

The typical measurements of neutrino features, such as oscillations, are based on the number of specific flavours of neutrinos that appear or disappear after a given distance from their production point, compared to the number of produced neutrinos. The future generation of neutrino oscillation experiments, such as HyperKamiokande and DUNE, will be no longer limited by statistics and will need to reduce the systematic uncertainties and in particular the one related to the neutrino cross section that, especially for the appearing species, the ν_e , is poorly known. In order to reduce this uncertainty, a new generation of neutrino beams has been proposed [2, 3].

The goal of the ENUBET project (Enhanced NeUtrino BEams from Kaon Tagging) is to develop the first *monitored neutrino beam*, where the neutrino flux can be measured with a 1% precision, in order to perform a high precision cross section measurement. The idea is to design a pure and controlled source of electron neutrinos and to monitor the neutrino flux directly inside the decay region by detecting large-angle leptons generated in the K_{e3}^+ three body decay ($K^+ \rightarrow e^+ \pi^0 \nu_e$) using sampling calorimeters based on plastic scintillators and placed inside the decay tunnel. Thus, the tunnel becomes a hollow cylindrical electromagnetic calorimeter with an inner radius of 1 m and a length of 40 m [4-8].

2. – The Demonstrator

The Demonstrator is a section of the ENUBET instrumented decay tunnel. This prototype is 1.65 m long and it is composed of 75 arches of iron alternated with 75 arches of plastic scintillators spanning 90° . This modular design could be extended then to a full 2π object. The Demonstrator is housed in a custom structure with four extendable legs allowing the calorimeter tilting (to simulate the impact of the large-angle positrons produced by the $K_{e_3}^+$ decay) as shown in fig. 1(a).

The iron components are made of single slabs, while the scintillating planes are segmented in all the three directions (the $3 \times 3 \times 0.7 \text{ cm}^3$ tiles) as shown in fig. 1(b). The tile scintillating light is collected by WaveLength Shifting (WLS) fibers and readout by Silicon PhotoMultipliers (SiPMs).

In order to detect positrons and distinguish them from photons, the two upstream active layers are instrumented with an additional tile placed in the innermost radial layer, the so called t_0 photon veto layer. Photons produced in the decay tunnel will not give a hit in the t_0 layer associated with an energy deposit in the calorimeter, and will not be misidentified as positrons.

In October 2022 and August 2023, the ENUBET collaboration performed a beamtest on the PS extracted T9 beamline at CERN. The main goals of these beamtests were to evaluate the performance of the Demonstrator which in 2022 consisted in 400 readout channels (240 calorimetric channels and 160 t_0 tiles) and in 2023 in 1275 channels.

3. – Linearity and energy resolution

Due to residual differences in the the optical coupling between the SiPM and the WLS fibers, an equalization procedure of the response of each channel is needed. For each channel, the Minimum Ionizing Particle (MIP) events have been selected whose mean energy loss rate through matter is constant. The MIP peak has been fitted with a Landau function and then every channel has been equalized subtracting the *baseline* value and then dividing for the MIP *peak*.

To find the correspondence between the Pulse Heights (PHs in ADC counts) and the energy deposited in the Demonstrator (in GeV) by the incoming particles, a calibration

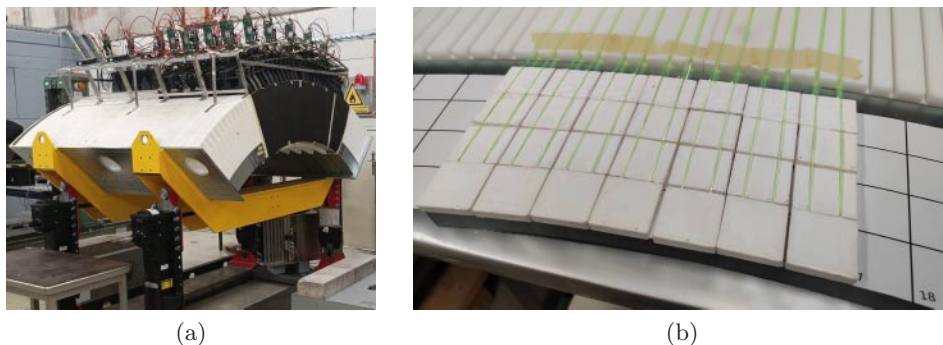


Fig. 1. – (a) The assembled Demonstrator at CERN. (b) An assembled arch with a plane of tiles. The innermost radial layer is the t_0 photon veto layer.

with electron beams was performed. The events were acquired with 0.5 GeV – 5 GeV (E_{GeV}) electron beams.

The equalized PH spectra of the events were fitted with a Gaussian function. The fit parameters allowed to compute the energy resolution for each energy $R = \sigma_E/E$, where E is the mean value and σ_E is the standard deviation of the Gaussian function.

A linear regression was performed on the (E_{GeV} , E) pairs and, to verify the goodness of the calibration, the residuals have been computed obtaining values smaller than 1%.

The dependence of the energy resolution on the beam energy (E_{GeV}) was modeled as [9]:

$$(1) \quad R = \frac{s}{\sqrt{E_{\text{GeV}}}} \oplus \frac{n}{E_{\text{GeV}}} \oplus c$$

where \oplus is the quadratic sum, s the stochastic term, n is the noise term and c the constant term. The resolution curves for the 2023 prototype and the Monte Carlo simulation, performed with the Geant4 toolkit, are shown in fig. 2.

4. – Crosstalk

Optical crosstalk occurs when the light produced in a scintillator tile travels to a neighbouring one and might then be picked up by one of its readout fibers. This would generate a signal in the wrong tile, affecting the performance of the calorimeter. The crosstalk effect has been studied only for the first layer (for both the Demonstrator prototypes) and with muon events which have a track in an area of $1 \times 1 \text{ cm}^2$ centered in the centre of a tile. Muons have been selected thanks to their MIP behavior, since they do not produce showers, as electrons and pions, which could produce a signal in adjacent tiles due to the secondary particles of the shower and not to crosstalk.

To better understand the crosstalk the mean value of the ratio between the PH of two channels has been computed:

$$(2) \quad \text{ratio}_{PH} = \langle (PH_2/PH_1) \rangle$$

where PH_1 is the reference channel with a PH greater than $0.7 \cdot MIP$ and PH_2 is a neighbouring channel of the same layer. Figure 3 presents an example where tile

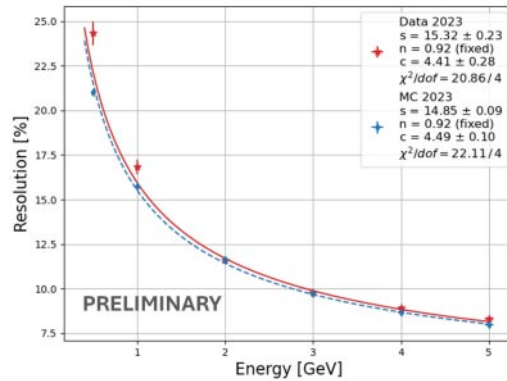


Fig. 2. – Energy resolution of the Demonstrator in the 0.5 – 5 GeV energy range.

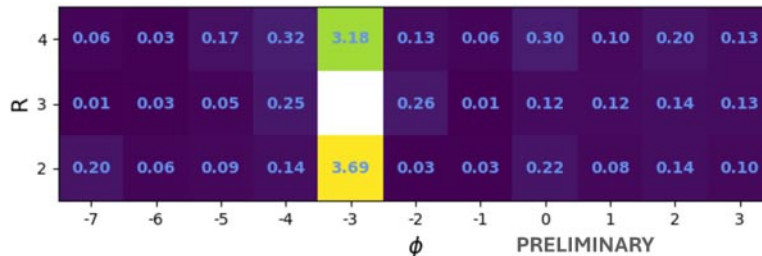


Fig. 3. – Crosstalk effect for tile $(3, -3, 0)$ as reference (white square).

$(R, \phi, z) = (3, -3, 0)$ is the reference tile and the $ratio_{PH}$ parameter is computed for all the other tiles of the first z layer. Most of the channels present a few percent of crosstalk and always smaller than 5% between closest tiles.

5. – Preliminary Particle Identification

For this analysis, the Demonstrator has been tilted with angles of 50 mrad, 100 mrad and 200 mrad to try to reproduce the particle incidence angle in the final configuration of the future ENUBET detector. These tilted angle runs with electron and hadron beams can be used to perform a preliminary Particle IDentification (PID) analysis, to tentatively estimate the PID capabilities of the final detector. This cut-based analysis is a basic and faster alternative to the more refined one that is based on a Neural Network and has been developed and applied in the simulation of the full facility.

Two parameters have been evaluated to define a way to identify the particle type: the total number of tiles over a given threshold and the sum of the PHs in all the z layers. Figure 4 presents the biplot of these two parameters. Three spots can be distinguished: the upper one is mainly composed of electron events (green circle of fig. 4), the middle one of heavy hadrons (orange circle of fig. 4) and the lower one of muons (red circle of fig. 4).

To distinguish electron events from heavy hadron ones, a linear cut was applied (red line in fig. 4). The events over this cut are classified as electrons and the ones under the cut as heavy hadrons. These events correspond to the *predicted value*, while the identification performed with the Cherenkov detectors was used as *true value*. To estimate the goodness of the classification, the accuracy and precision⁽¹⁾ were computed, obtaining an accuracy of 78.27% and a precision of 73.28% in classifying electrons and an accuracy of 76.74% and a precision of 87.91% in classifying heavy hadrons.

6. – Conclusions and outlooks

In October 2022 and August 2023, the ENUBET collaboration performed a beamtest on the PS extracted T9 beamline at CERN to evaluate the performance of the Demonstrator. The crosstalk effect has been studied for the first z layer and measured values of

⁽¹⁾ The accuracy of a measurement system is the degree of closeness of the measured quantity to its true value. The precision of a measurement system is how close the measurements are to each other [10].

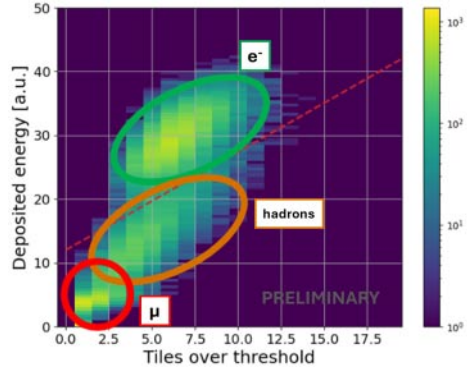


Fig. 4. – Biplot of the two parameters used for a preliminary PID. The red line is the linear cut to distinguish electrons from heavy hadrons and muons.

a few percent ($< 5\%$) between neighbour tiles have been obtained. This result allowed to validate the proposed readout scheme. Finally, the preliminary results on the PID capability of the Demonstrator show how, even with an extremely basic discrimination, it is already possible to distinguish electrons and heavy hadrons.

Based on these successful results, the collaboration is now pursuing a study for a site dependent implementation at CERN in the framework of Physics Beyond Colliders using the SPS as proton driver and the two protoDUNE detectors as neutrino detector.

* * *

This project has received funding from the European Union Horizon 2020 Research and Innovation programme under Grant Agreement No. 681647 and the Italian Ministry for Education and Research (MIUR, bando FARE, progetto NUTECH, R1623F4S38). It is also supported by the Agence Nationale de la Recherche (ANR, France) through the PIMENT project (ANR-21-CE31-0027) and by the Ministry of Science and Education of Republic of Croatia grant No. KK.01.1.1.01.0001.

REFERENCES

- [1] CAMILLERI L., *Neutrino Detectors*, in *Particle Physics Reference Library: Volume 2: Detectors for Particles and Radiation*, edited by FABJAN C. W. and SCHOPPER H. A. (Springer International Publishing) 2020, pp. 337–382.
- [2] CHARITONIDIS N., LONGHIN A., PARI M., PAROZZI E. G., and TERRANOVA F., *Appl. Sci.*, **11** (2021) 1644.
- [3] BRANCA A., BRUNETTI G., LONGHIN A., MARTINI M., PUPILLI F. and TERRANOVA F., *Symmetry*, **13** (2021) 9.
- [4] LONGHIN A., LUDOVICI L and TERRANOVA F., *Eur. Phys. J. C*, **75** (2015) 155.
- [5] LONGHIN A. and TERRANOVA F., CERN-SPSC-2020-009, SPSC-SR-268.
- [6] ACERBI F. *et al.*, CERN-SPSC-2021-013, SPSC-SR-290.
- [7] ACERBI F. *et al.*, CERN-SPSC-2022-016, SPSC-SR-310.
- [8] ACERBI F. *et al.*, *Eur. Phys. J. C*, **83** (2023) 964.
- [9] FABJAN C. W. and GIANOTTI F., *Rev. Mod. Phys.*, **75** (2003) 1243.
- [10] TAYLOR J. R., *An Introduction to Error Analysis. The Study of Uncertainties in Physical Measurements*, 2nd edition (University Science Books) 1982, pp. 337–382.